

# Nanostructuring of PEDOT in Porous Coordination Polymers for Tunable Porosity and Conductivity

Benjamin Le Ouay,<sup>†,‡</sup> Mickael Boudot,<sup>§</sup> Takashi Kitao,<sup>†</sup> Takeshi Yanagida,<sup>§</sup> Susumu Kitagawa,<sup>\*,†,#</sup> and Takashi Uemura<sup>\*,†,‡</sup>

<sup>†</sup>Department of Synthetic Chemistry and Biological Chemistry, Graduate School of Engineering, Kyoto University, Katsura, Nishikyo-ku, Kyoto 615-8510, Japan

<sup>‡</sup>CREST, Japan Science and Technology Agency (JST), 4-1-8 Honcho, Kawaguchi, Saitama 332-0012, Japan

<sup>§</sup>Institute for Materials Chemistry and Engineering, Kyushu University, 6-1 Kasuga-Koen, Kasuga, Fukuoka 816-8580, Japan

<sup>#</sup>Institute for Integrated Cell-Material Sciences (WPI-iCeMS), Kyoto University, Yoshida, Sakyo-ku, Kyoto 606-8501, Japan

## Supporting Information

**ABSTRACT:** A series of conductive porous composites were obtained by the polymerization of 3,4-ethylenedioxythiophene (EDOT) in the cavities of MIL-101(Cr). By controlling the amount of EDOT loaded into the host framework, it was possible to modulate the conductivity as well as the porosity of the composite. This approach yields materials with a reasonable electronic conductivity ( $1.1 \times 10^{-3} \text{ S}\cdot\text{cm}^{-1}$ ) while maintaining high porosity ( $S_{\text{BET}} = 803 \text{ m}^2/\text{g}$ ). This serves as a promising strategy for obtaining highly nanotextured conductive polymers with very high accessibility for small gas molecules, which are beneficial to the fabrication of a chemiresistive sensor for the detection of  $\text{NO}_2$ .

Over the past two decades, porous coordination polymers (PCPs), also known as metal-organic frameworks (MOFs), have appeared as a promising and versatile class of materials.<sup>1-3</sup> Their success is largely due to their exceptional characteristics, among which are very high porosity, a variety of topologies, and tunability of their properties through selection of the metal centers or ligands or inclusion of guests. However, applications of PCPs in the field of electrochemistry remain scarce, especially when excluding the field of ion-conductive networks.<sup>4,5</sup> The main reason for this is the lack of electronic conductivity of most frameworks, with only a few PCPs reported as electron conductors.<sup>6-12</sup> Because they have active metal centers easily accessed by diffusive species and electrons, these materials possess excellent electrochemical properties, as demonstrated by recent reports.<sup>13-16</sup> Unfortunately, and without denying the impressive properties of compounds already (and to-be) described, this class of materials suffers from limited tunability, as small changes in the nature of the metal or ligand resulted in a significant decrease in their conductivity.<sup>17-19</sup> Furthermore, because high electronic conduction requires multiple conduction pathways, the porosity of this category of PCPs remains relatively low.

To benefit from both the versatility of PCPs' functionality and the electronic conduction, we propose to synthesize conductive polymers such as poly(3,4-ethylenedioxythiophene) (PEDOT)<sup>20</sup> in the pores of a PCP. Similar approaches have

already been reported to prepare conductive polymer chains in one-dimensional (1-D) nanochannels,<sup>21-23</sup> 2-D nanoslits,<sup>24</sup> and 3-D pores.<sup>25-27</sup> However, PCP/polymer composites with reasonably high porosity as well as conductivity have yet to be prepared. To obtain conduction isotropy and mass transport in the occupied pores, we used a 3-D PCP,  $[\text{Cr}_3(\text{BDC})_3\text{OF}(\text{H}_2\text{O})_2]_n$  (MIL-101(Cr), BDC = benzenedicarboxylate),<sup>28</sup> denoted as **1**. This PCP is readily available at the gram scale, highly porous, and widely studied along with its functional variants.<sup>29,30</sup>

Composite materials between **1** and PEDOT were prepared in two steps (Figure 1). First, a controlled amount (chosen below the maximal loading capacity) of 3,4-ethylenedioxythiophene (EDOT) dissolved in diethyl ether was introduced into the host PCP by evaporation of the solvent. This approach allowed a homogeneous dispersion of monomers throughout **1** as well as a precise control of the loading rate. Owing to the very high porosity of **1**, the maximum EDOT loading was estimated to be  $160 \pm 10\%$  of the empty PCP mass, a value comparable to that of ibuprofen (density: 1.03; 140 wt %).<sup>31</sup>

The second step consisted of the oxidative polymerization of EDOT in the pores of **1** by iodine vapors.<sup>32</sup> Unlike other common oxidizers (e.g.,  $\text{FeCl}_3$  and persulfate), iodine can easily be sublimed and allow reaction between a gaseous reagent and the monomers adsorbed on the pore walls inside the PCP. Note that after evacuation of the unreacted  $\text{I}_2$ , PEDOT remained in a highly doped (and thus conductive) state, with ionic iodine species acting as the counterions.

Preservation of the PCP framework during the polymerization was confirmed by powder X-ray diffraction (PXRD), which indicated the presence of characteristic peaks of **1** (Figure 2). Differences in the relative intensities of the peaks after the polymerization can be explained by the presence of disordered guest polymer chains in the pores<sup>33</sup> and is especially strong in our case as iodine species are strong X-ray scatterers.

Formation of PEDOT and elimination of unreacted EDOT were assessed using ATR-FTIR (Supporting Information). MALDI-TOF indicated the presence of oligomers having molecular weight up to 1286 Da. Meanwhile, number-average

Received: June 7, 2016

Published: August 2, 2016

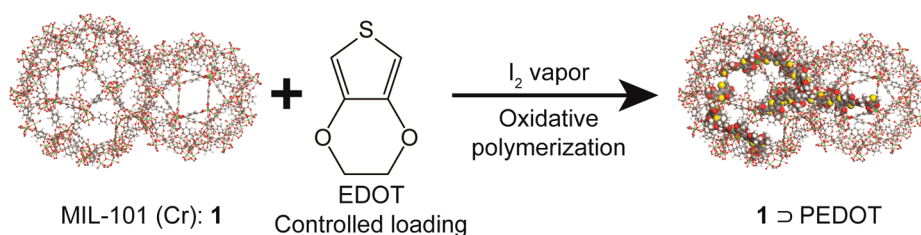


**Figure 1.** Schematic image for the preparation of **1@PEDOT**.

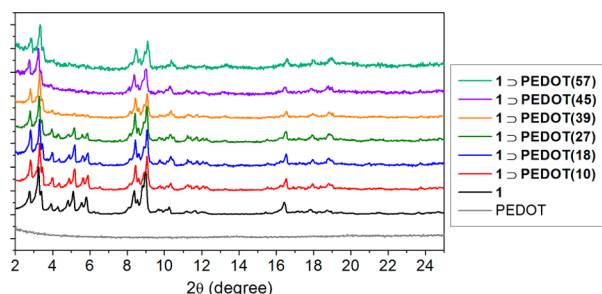


**Figure 2.** XRD diagrams of pristine PEDOT, **1**, and **1@PEDOT**. The number in the parentheses indicates the mass fraction of PEDOT in the sample.

molecular weight  $M_n$  was determined as 2960 Da by gel permeation chromatography (GPC). Discrepancies between both techniques are discussed in [Supporting Information](#). The polymerization yield was estimated using XRF, based on the S/Cr ratio. The polymerization yield was between 82% and 86% for all samples, indicating the high reactivity of EDOT in the porous network. In this study, we designate composites as **1@PEDOT**-(*X*), where *X* is the mass fraction of PEDOT in the composite (determined from the S/Cr ratio by XRF). *X* could be varied in **1** from 10% to 57% depending on the amount of EDOT loaded.

The porosity of the composites were assessed by adsorption of  $N_2$  at 77 K ([Figure 3A](#)). Pristine host PCP **1** possessed a specific surface area  $S_{BET}$  of  $\sim 3100 \text{ m}^2/\text{g}$ .<sup>28,30</sup> As expected,  $S_{BET}$  of

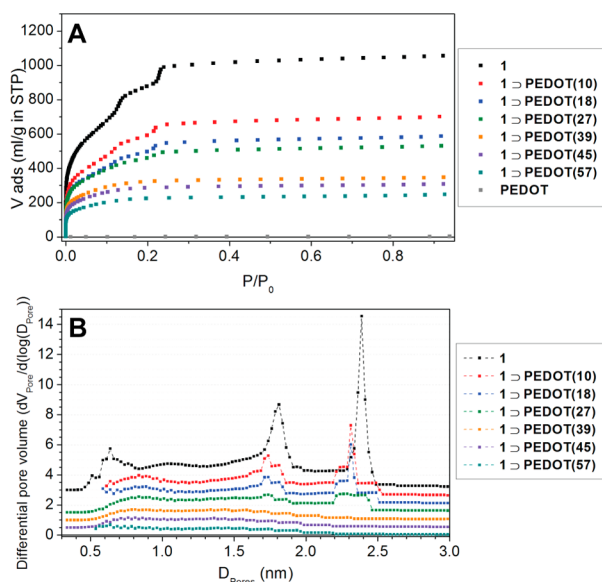


**Figure 3.** (A) Adsorption isotherms ( $N_2$ , 77 K) of **1** and **1@PEDOT**. (B) HK plot of **1** and **1@PEDOT** composites. An offset of 0.5 between each curve was added for readability.

**1@PEDOT** decreased as the loading rate increased. However, due to the high porosity of the host material, the value of  $S_{BET}$  at high loading still remained reasonably high. For example,  $S_{BET}$  of **1@PEDOT**(57) was calculated as  $803 \text{ m}^2/\text{g}$ , which is higher than any conductive PCP reported so far. **1@PEDOT** presented a type I isotherm, indicative of microporosity. The micropore size distribution, determined using the HK (Horváth and Kawazoe) method<sup>34</sup> ([Figure 3B](#)), indicated the presence of two types of pores in **1** with diameters of 1.8 and 2.3 nm, corresponding to the two types of cages. For low loading rates, the apparent diameter of the cages decreased slightly, indicating that the polymer formed close to the pore walls, while the volume in the cages remained accessible.

For high loading, the stacking of several PEDOT layers on the pore walls decreased the apparent pore diameter. However, the composites maintained a broad distribution of pores with diameters between 0.5 and 2.2 nm. Raman spectroscopy and molecular dynamics (MD) simulations indicated that PEDOT presented a coiled structure with a low degree of order for the chains ([Supporting Information](#)). This effect was attributed to the curvature of the cage walls that prevented ordering of the PEDOT chains over long distances.

Conductivity was measured using impedance spectroscopy (two electrodes) on pressure-sintered pellets. Pristine **1** exhibited almost no conductivity ( $\sigma < 10^{-11} \text{ S}\cdot\text{cm}^{-1}$ ), as expected from the absence of electron-conduction paths. In contrast, the impedance diagrams of **1@PEDOT** had the shape of a semicircle when plotted in the Nyquist representation and impedance reached a pure real value at low frequency ([Supporting Information](#)). This was attributed to an electronic conduction through the PEDOT network, with iodine species acting as a dopant. The conductivities of **1@PEDOT**, as well as  $S_{BET}$  are reported in [Figure 4](#). The conductivity of the composites increased greatly with the PEDOT weight fraction. For the highest loading rate (**1@PEDOT**(57)), the conductivity reached a value of  $1.1 \times 10^{-3} \text{ S}\cdot\text{cm}^{-1}$ . This value was higher than those of the composites between **1** and other conducting polymers, such as unsubstituted polythiophene and polypyrrole, prepared in the

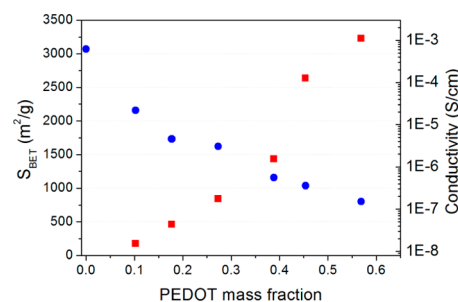


**Figure 4.** Conductivity (red squares) and specific surface area (blue circles) of **1@PEDOT**.

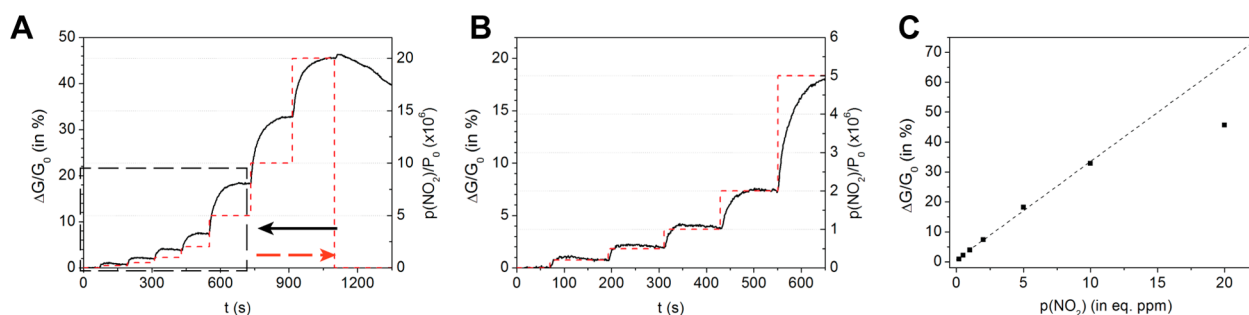


**Figure 5.** (A) Time-dependent variations of conductivity of a chemiresistive sensor prepared using 1D PEDOT(45) (plain line, left axis) under different partial pressures of  $\text{NO}_2$  (dashed, right axis). (B) Zoom-in on the low-pressure domain. (C) Linear fit of the conductivity changes as a function of the partial pressure of  $\text{NO}_2$ .

similar manner, indicating the significant role of the conductive polymer's nature (Supporting Information). We also prepared PEDOT in 1-D channels of  $\text{La}(1,3,5\text{-benzenetrisbenzoate})$ ,<sup>35</sup> where the conductivity of the composite (30 wt % PEDOT) was much lower ( $2.3 \times 10^{-8} \text{ S}\cdot\text{cm}^{-1}$ ) than for corresponding 1D PEDOT, probably because of the low interchain connectivity of PEDOT isolated in the 1-D nanochannels (Supporting Information). This indicates the essential role of the topology of the PCP's pores for the design of a conductive composite. While the conductivity of 1D PEDOT was lower than the highest values published for conductive PCPs,<sup>10</sup> it is still appreciable and allows application in electrochemistry.

PEDOT is a *p*-type semiconductor and its Fermi level can be modified by the presence of oxidizing analytes, resulting in measurable changes of its conductivity. For this reason, PEDOT has often been used for the chemiresistive detection of  $\text{NO}_2$ .<sup>36–40</sup> The detection of this analyte is of very great importance, as it is a common atmospheric pollutant produced during combustion reactions, with a toxic effect on the respiratory system at concentrations of 1 ppm and below.<sup>41</sup> Thus, we initially prepared a  $\text{NO}_2$  sensor using conventional bulk PEDOT obtained from solution polymerization. However, this PEDOT sensor presented a significant drift, along with a very low sensitivity (0.8% for a partial pressure of  $\text{NO}_2$   $P(\text{NO}_2) = 1 \text{ Pa}$ , equivalent to 10 ppm), probably because of low accessibility for gas analytes ( $S_{\text{BET}}$  of pristine PEDOT =  $2 \text{ m}^2/\text{g}$ ). Because the design of microporous and conductive materials is highly sought after to achieve efficient gas sensors,<sup>13,42–44</sup> preparation of PEDOT in **1** is a reasonable strategy to induce a nanostructuring of PEDOT, which could develop a very high accessible surface area. As conductive polymer chains tend to aggregate because of  $\pi$ -stacking, their structuration at the subnanometer scale (where chains are isolated or form bundles of a few entities) is so far only attainable by molecular engineering of the side-chains.<sup>45,46</sup> Here, we employed 1D PEDOT(45) ( $S_{\text{BET}} = 1038 \text{ m}^2/\text{g}$ ) for chemiresistive sensing of  $\text{NO}_2$  gas. This composite presented the best compromise between high conductivity to reduce the effect of electrical noise and high accessibility for gas molecules. As seen in Figure 5A,B, the conductivity of the sensor increased sharply when put in contact with  $\text{NO}_2$ . The response time to reach the equilibrium state was below 30 s for low partial pressures and remained below 150 s for  $P(\text{NO}_2)$  up to 20 ppm. The conductivity increase was found to be linear ( $R^2 = 0.9974$ ) for  $P(\text{NO}_2)$  up to 10 ppm (Figure 5C). The minimum  $P(\text{NO}_2)$  measured was 200 ppb, with a sensor response of 0.9%. Considering the linearity slope  $\alpha$  and the electrical noise standard deviation  $\delta$ , the limit of detection (LOD) at  $3\delta$  was estimated at 60 ppb. Being operated at room temperature and having a high

sensitivity, a low LOD, and a wide linearity range, the performances of our sensing device were very promising compared with other systems based on nanostructured conducting polymers<sup>38–42</sup> and were indeed close to the most efficient and optimized PEDOT-based sensors for  $\text{NO}_2$ , which rely on the modulation of a *p*–*n* junction instead of a direct Fermi level modification.<sup>47,48</sup>

In summary, we have produced a series of porous electronic conductors based on the polymerization of EDOT in **1**, which possesses a 3-D porous structure. By varying the amount of monomer introduced in the pores, it was possible to modulate the conductivity as well as the porosity of the composites. The conductivity of 1D PEDOT reached  $1.1 \times 10^{-3} \text{ S}\cdot\text{cm}^{-1}$  with the highest loading of the polymer, while the specific surface area remained as high as  $803 \text{ m}^2/\text{g}$ . Furthermore, we deliberately chose an archetypal PCP framework, as a proof-of-concept. Preparation of PCP/conductive polymer composites thus appears as a promising and versatile approach to obtain highly functional porous conductive materials. We have demonstrated the potential of this approach by producing a chemiresistive sensor that proved very efficient for the detection of  $\text{NO}_2$ .

## ■ ASSOCIATED CONTENT

### Supporting Information

The Supporting Information is available free of charge on the ACS Publications website at DOI: 10.1021/jacs.6b05552.

Synthetic procedure and additional characterizations (PDF)

## ■ AUTHOR INFORMATION

### Corresponding Authors

\*uemura@sbchem.kyoto-u.ac.jp

\*kitagawa@icems.kyoto-u.ac.jp

### Notes

The authors declare no competing financial interest.

## ■ ACKNOWLEDGMENTS

This work was supported by the JST, CREST program, and a Grant-in Aid for Science Research on Innovative Area “New Polymeric Materials Based on Element-Blocks” (No. 2401) from the Ministry of Education, Culture, Sports, Science and Technology, Government of Japan.

## ■ REFERENCES

- (1) Kitagawa, S.; Kitaura, R.; Noro, S. *Angew. Chem., Int. Ed.* **2004**, *43*, 2334.
- (2) Ferey, G. *Chem. Soc. Rev.* **2008**, *37*, 191.



- (3) Furukawa, H.; Cordova, K. E.; O'Keeffe, M.; Yaghi, O. M. *Science* **2013**, *341*, 974.
- (4) Morozan, A.; Jaouen, F. *Energy Environ. Sci.* **2012**, *5*, 9269.
- (5) Xia, W.; Mahmood, A.; Zou, R.; Xu, Q. *Energy Environ. Sci.* **2015**, *8*, 1837.
- (6) Givaja, G.; Amo-Ochoa, P.; Gomez-Garcia, C. J.; Zamora, F. *Chem. Soc. Rev.* **2012**, *41*, 115.
- (7) Sun, L.; Campbell, M. G.; Dincă, M. *Angew. Chem., Int. Ed.* **2016**, *55*, 3566.
- (8) Takaishi, S.; Hosoda, M.; Kajiwara, T.; Miyasaka, H.; Yamashita, M.; Nakanishi, Y.; Kitagawa, Y.; Yamaguchi, K.; Kobayashi, A.; Kitagawa, H. *Inorg. Chem.* **2009**, *48*, 9048.
- (9) Talin, A. A.; Centrone, A.; Ford, A. C.; Foster, M. E.; Stavila, V.; Haney, P.; Kinney, R. A.; Szalai, V.; El Gabaly, F.; Yoon, H. P.; Léonard, F.; Allendorf, M. D. *Science* **2014**, *343*, 66.
- (10) Sheberla, D.; Sun, L.; Blood-Forsythe, M. A.; Er, S.; Wade, C. R.; Brozek, C. K.; Aspuru-Guzik, A.; Dincă, M. *J. Am. Chem. Soc.* **2014**, *136*, 8859.
- (11) Darago, L. E.; Aubrey, M. L.; Yu, C. J.; Gonzalez, M. I.; Long, J. R. *J. Am. Chem. Soc.* **2015**, *137*, 15703.
- (12) Chen, D.; Xing, H.; Su, Z.; Wang, C. *Chem. Commun.* **2016**, *52*, 2019.
- (13) Campbell, M. G.; Sheberla, D.; Liu, S. F.; Swager, T. M.; Dincă, M. *Angew. Chem., Int. Ed.* **2015**, *54*, 4349.
- (14) Campbell, M. G.; Liu, S. F.; Swager, T. M.; Dincă, M. *J. Am. Chem. Soc.* **2015**, *137*, 13780.
- (15) Aubrey, M. L.; Long, J. R. *J. Am. Chem. Soc.* **2015**, *137*, 13594.
- (16) Miner, E. M.; Fukushima, T.; Sheberla, D.; Sun, L.; Surendranath, Y.; Dincă, M. *Nat. Commun.* **2016**, *7*, 10942.
- (17) Kobayashi, Y.; Jacobs, B.; Allendorf, M. D.; Long, J. R. *Chem. Mater.* **2010**, *22*, 4120.
- (18) Park, S. S.; Hontz, E. R.; Sun, L.; Hendon, C. H.; Walsh, A.; Van Voorhis, T.; Dincă, M. *J. Am. Chem. Soc.* **2015**, *137*, 1774.
- (19) Sun, L.; Hendon, C. H.; Minier, M. A.; Walsh, A.; Dincă, M. *J. Am. Chem. Soc.* **2015**, *137*, 6164.
- (20) Kirchmeyer, S.; Reuter, K. *J. Mater. Chem.* **2005**, *15*, 2077.
- (21) Wang, Q.-X.; Zhang, C.-Y. *Macromol. Rapid Commun.* **2011**, *32*, 1610.
- (22) Uemura, T.; Uchida, N.; Asano, A.; Saeki, A.; Seki, S.; Tsujimoto, M.; Isoda, S.; Kitagawa, S. *J. Am. Chem. Soc.* **2012**, *134*, 8360.
- (23) MacLean, M. W. A.; Kitao, T.; Suga, T.; Mizuno, M.; Seki, S.; Uemura, T.; Kitagawa, S. *Angew. Chem.* **2016**, *128*, 718.
- (24) Yanai, N.; Uemura, T.; Ohba, M.; Kadowaki, Y.; Maesato, M.; Takenaka, M.; Nishitsuji, S.; Hasegawa, H.; Kitagawa, S. *Angew. Chem., Int. Ed.* **2008**, *47*, 9883.
- (25) Uemura, T.; Kadowaki, Y.; Yanai, N.; Kitagawa, S. *Chem. Mater.* **2009**, *21*, 4096.
- (26) Lu, C.; Ben, T.; Xu, S.; Qiu, S. *Angew. Chem., Int. Ed.* **2014**, *53*, 6454.
- (27) Aliev, S. B.; Samsonenko, D. G.; Maksimovskiy, E. A.; Fedorovskaya, E. O.; Sapchenko, S. A.; Fedin, V. P. *New J. Chem.* **2016**, *40*, 5306.
- (28) Férey, G.; Mellot-Draznieks, C.; Serre, C.; Millange, F.; Dutour, J.; Surblé, S.; Margiolaki, I. *Science* **2005**, *309*, 2040.
- (29) Hong, D.-Y.; Hwang, Y. K.; Serre, C.; Férey, G.; Chang, J.-S. *Adv. Funct. Mater.* **2009**, *19*, 1537.
- (30) Zhao, T.; Jeremias, F.; Boldog, I.; Nguyen, B.; Henninger, S. K.; Janiak, C. *Dalton Trans.* **2015**, *44*, 16791.
- (31) Horcajada, P.; Serre, C.; Vallet-Regí, M.; Sebban, M.; Taulelle, F.; Férey, G. *Angew. Chem.* **2006**, *118*, 6120.
- (32) Bhattacharyya, D.; Howden, R. M.; Borrelli, D. C.; Gleason, K. K. *J. Polym. Sci., Part B: Polym. Phys.* **2012**, *50*, 1329.
- (33) Hafizovic, J.; Bjørgen, M.; Olsbye, U.; Dietzel, P. D. C.; Bordiga, S.; Prestipino, C.; Lamberti, C.; Lillerud, K. P. *J. Am. Chem. Soc.* **2007**, *129*, 3612.
- (34) Horvath, G.; Kawazoe, K. *J. Chem. Eng. Jpn.* **1983**, *16* (6), 470.
- (35) Devic, T.; Serre, C.; Audebrand, N.; Marrot, J.; Férey, G. *J. Am. Chem. Soc.* **2005**, *127*, 12788.
- (36) Bai, H.; Shi, G. *Sensors* **2007**, *7*, 267.
- (37) Pinto, N. J.; Rivera, D.; Melendez, A.; Ramos, I.; Lim, J. H.; Johnson, A. T. *C. Sens. Actuators, B* **2011**, *156*, 849.
- (38) Yang, Y.; Li, S.; Yang, W.; Yuan, W.; Xu, J.; Jiang, Y. *ACS Appl. Mater. Interfaces* **2014**, *6*, 13807.
- (39) Shaik, M.; Rao, V. K.; Sinha, A. K.; Murthy, K. S. R. C.; Jain, R. J. *Environ. Chem. Eng.* **2015**, *3*, 1947.
- (40) Dunst, K.; Jurkó, D.; Jasiński, P. *Sens. Actuators, B* **2016**, *229*, 155.
- (41) Hesterberg, T. W.; Bunn, W. B.; McClellan, R. O.; Hamade, A. K.; Long, C. M.; Valberg, P. A. *Crit. Rev. Toxicol.* **2009**, *39*, 743.
- (42) Travlou, N. A.; Singh, K.; Rodriguez-Castellon, E.; Bandosz, T. J. *J. Mater. Chem. A* **2015**, *3*, 11417.
- (43) Wisser, F. M.; Grothe, J.; Kaskel, S. *Sens. Actuators, B* **2016**, *223*, 166.
- (44) Nguyen, N. D.; Yoon, H. *Polymers* **2016**, *8*, 118.
- (45) Rose, A.; Zhu, Z.; Madigan, C. F.; Swager, T. M.; Bulovic, V. *Nature* **2005**, *434*, 876.
- (46) Pan, C.; Zhao, C.; Takeuchi, M.; Sugiyasu, K. *Chem. - Asian J.* **2015**, *10*, 1820.
- (47) Zampetti, E.; Pantalei, S.; Muzyczuk, A.; Bearzotti, A.; De Cesare, F.; Spinella, C.; Macagnano, A. *Sens. Actuators, B* **2013**, *176*, 390.
- (48) Hangarter, C. M.; Chartuprayoon, N.; Hernández, S. C.; Choa, Y.; Myung, N. V. *Nano Today* **2013**, *8*, 39.